

Exploring Filter Banks and Spike Interval Statistics of Level-Crossing ADCs for Fault Diagnosis of Rolling Element Bearings

Ashwani Kumar¹, Daniel Strömbergsson², Pär Marklund³, and Fredrik Sandin⁴

^{1,3}*Division of Machine Elements, Luleå University of Technology, Luleå, 97187, Sweden*

ashwani.kumar@associated.ltu.se
par.marklund@ltu.se

^{2,4}*Machine Learning Group - EISLAB, Luleå University of Technology, 97187, Luleå, Sweden*

daniel.strombergsson@ltu.se
fredrik.sandin@ltu.se

ABSTRACT

Nowadays, lots of data are generated in industries using vibration sensors to evaluate the equipment's working condition and identify faults. A significant challenge is that only a small fraction of data can be transmitted for intelligent fault diagnosis and storage. The edge processing capacity is often insufficient for advanced analysis due to time and resource constraints. The neuromorphic signal encoding scheme efficiently reduces the data rate by encoding relevant signal changes into spike trains while discarding redundant information and noise, enabling energy-efficient neuromorphic processing. Due to the presence of dominant operational features and noise in the original measurements, signal pre-processing is required to extract the relevant features before spike coding and processing. The work investigates the effects of different filter banks (pre-processing methods) on the spike encodings for vibration measurements from bearings. This also includes bearing fault features diagnosis based on statistical analysis of generated spikes. The comparative analysis is made for benchmarking different signal pre-processing methods (e.g., envelope, empirical mode decomposition (EMD), and gammatone filter) on bearing vibration datasets. An event-triggered scheme, i.e., Level-crossing analog-to-digital converters (LC-ADCs) is applied to encode the vibration measurement to spikes. Inter-spike intervals (ISIs) statistics are analysed for fault diagnosis of bearings. The results obtained for CWRU bearing databases indicate a possible fault detection and diagnosis with significant data rate reduction and an opportunity for improved computational efficiency. With the developed approach, the envelope filter is found to be the most efficient of all. This work enables a new approach to

Ashwani Kumar et al. This is an open-access article distributed under the terms of the Creative Commons Attribution 3.0 United States License, which permits unrestricted use, distribution, and reproduction in any medium, provided the original author and source are credited.

improve the energy efficiency of condition monitoring systems and further sets a new course of research development in this area using neuromorphic technologies.

1. INTRODUCTION

Machine condition monitoring plays a crucial role in today's fiercely competitive market. It serves as a powerful tool for industrial systems to fine-tune their management strategies (condition-based maintenance, remaining useful lifetime, degradation status, and environmental factors) and streamline their processes, enabling them to stay ahead of the competition (Ingemarsdotter et al., 2021). Therefore, it also brings a wealth of benefits to the industrial sector. By swiftly identifying potential equipment failures, it acts as a proactive guardian, preventing costly breakdowns and reducing unplanned downtime. Moreover, it is a cost-saving protector, helping industrial systems optimize maintenance efforts and allocate resources wisely. The global machine condition monitoring market is projected to soar to USD 4 billion by 2027, driven by escalating demand from oil and gas, power generation, and automotive industries (MarketsandMarkets, 2023). Machine condition monitoring systems led to a remarkable 24% drop in unplanned downtime (Ault & Bradley, 2022a) and a significant 10-25% decrease in maintenance expenses (uit het Broek et al., 2021; Yeadley et al., 2022).

Vibration analysis is a widely employed tool for condition monitoring of rotating machinery (Strömbergsson et al., 2020). It enables the early detection of faults and ensures optimal operational efficiency. By utilizing vibration analysis, machinery health can be continuously monitored, enabling the identification of fault signatures associated with issues such as misalignment, unbalance, bearing wear, or gear damage (de Sá Só Martins et al., 2021; Mohammed & Rantatalo, 2020; Strömbergsson et al., 2021).

The recent advancement in data-driven models for machine condition monitoring relies on the richness of available information within measured data to uncover insights about the underlying process (Nguyen et al., 2022; Quiñones-Grueiro et al., 2019). Vibration-bearing datasets, including FEMTO-ST, IMS, XJTU, CWRU, MPFT, and Paderborn, provide a wide range of fault scenarios and realistic vibration signals (Smith & Randall, 2015a; X. Zhang et al., 2021). These datasets are invaluable resources for evaluating and enhancing diagnostic methods, thereby facilitating algorithm development and comparative studies in the field of condition monitoring for bearings (Kumar et al., 2022; Sahu & Rai, 2022; Wang et al., 2023; Zabin et al., 2023).

Applying appropriate filtering techniques and noise reduction algorithms during data pre-processing significantly improves the quality and reliability of the signal analysis process (Yu et al., 2022). Filtering techniques have demonstrated their effectiveness in vibration signal analysis, with a proven track record supported by numerous studies. Various methods, such as the fast kurtogram, WPT, empirical mode decomposition (EMD), envelope, gammatone, and blind filters, are widely utilized in this field to enhance the understanding and interpretation of vibration signals. These techniques effectively enhance the comprehension of vibration signals, leading to accurate fault detection and reliable condition monitoring (Antoni, 2021a; Miao et al., 2022; Peeters et al., 2020; Sahu & Rai, 2022; K. Zhang et al., 2021).

The advent of Industry 4.0 has revolutionized industrial processes, leading to a significant increase in the adoption of machine learning practices. (Ahmer et al., 2022; Attoui et al., 2020; Hoang & Kang, 2019; Kuncan et al., 2020; D. Zhang et al., 2021; Zuo et al., 2022) The increasing interest in “black-box” solutions can be attributed to their robustness and high performance in tackling complex and nonlinear problems (Hoang & Kang, 2019). The application of these solutions brings significant benefits to industries, including optimized maintenance activities, improved equipment uptime, reduced operating costs, and enhanced overall operational efficiency (Ault & Bradley, 2022b; uit het Broek et al., 2021; Yearley et al., 2022). The development of advanced statistical and intelligent predictive maintenance techniques aims to optimize the diagnostic approach by leveraging recorded data. In the practice of continuous monitoring and earlier diagnosis, where the handling of large volumes of data is essential, energy plays a crucial role. Key components involved in this process include sensors for data capture, wired or wireless (WLAN/Zigbee/Bluetooth) connections for data transmission, filters for pre-processing, and GPU for efficient data analysis. The energy expenditure on condition monitoring in industries is also increasing every year with the increase in its market size (CAGR rate of 7.8 % from 2022 to 2027 (MarketsandMarkets, 2023)).

In monitoring systems, on-chip feature extraction and compression techniques are applied after sampling signals from an analog-to-digital converter (ADC) (Deepu et al., 2018; Dennler et al., 2021; Li et al., 2020). A recent advancement in ADC technology is the development of level-crossing ADCs (LC-ADCs), which integrate compression during the data acquisition stage (Saeed et al., 2021; Van Assche & Gielen, 2020). This approach is gaining interest in converting continuous signals to neural spikes (spike data), as it effectively reduces on-chip bandwidth and energy consumption (Saeed et al., 2021). However, to date there is no comparison of the effect of different filter-bank choices on the signal representation obtained with LC-ADCs for energy-efficient bearing condition monitoring purposes.

This work investigates alternative methods to generate a succinct event-based representation of condition monitoring vibration signals, e.g., enabling low-power edge processing applications. The main contributions are:

1. Comparison of EMD, Envelope, and Gammatone filter banks for signal decomposition.
2. Application of LC-ADCs for spike coding of the decomposed vibration signals (transforming time domain signals to spike trains).
3. Fault diagnosis based on spike timing analysis using inter-spike interval histograms.

The schematic representation of the workflow is given in Figure 1.

2. DATA AND DECOMPOSITION

Vibration-based machine condition monitoring relies on dataset selection and pre-processing techniques to extract relevant fault features. The Case Western Reserve University (CWRU) dataset is utilized in this study, and three different filter banks are employed for signal decomposition. The objective is to compare and identify the most suitable filter bank for vibration analysis using spike encoding, prioritizing reduced latency and energy consumption.

2.1. Dataset

The Case Western Reserve University (CWRU) vibration dataset is widely recognized and utilized for machine learning in fault diagnosis and prognostics of rotating machinery (Loparo, 2012). The dataset specifically emphasizes the bearings of the electric motor main shaft, which is connected to a dynamometer for generating braking torque. One of the motor bearings, an SKF deep groove ball bearing of type 6205-2RS JEM, is employed for testing. During data acquisition, accelerometers are strategically placed on the motor housing to capture vibrations across various operating conditions.

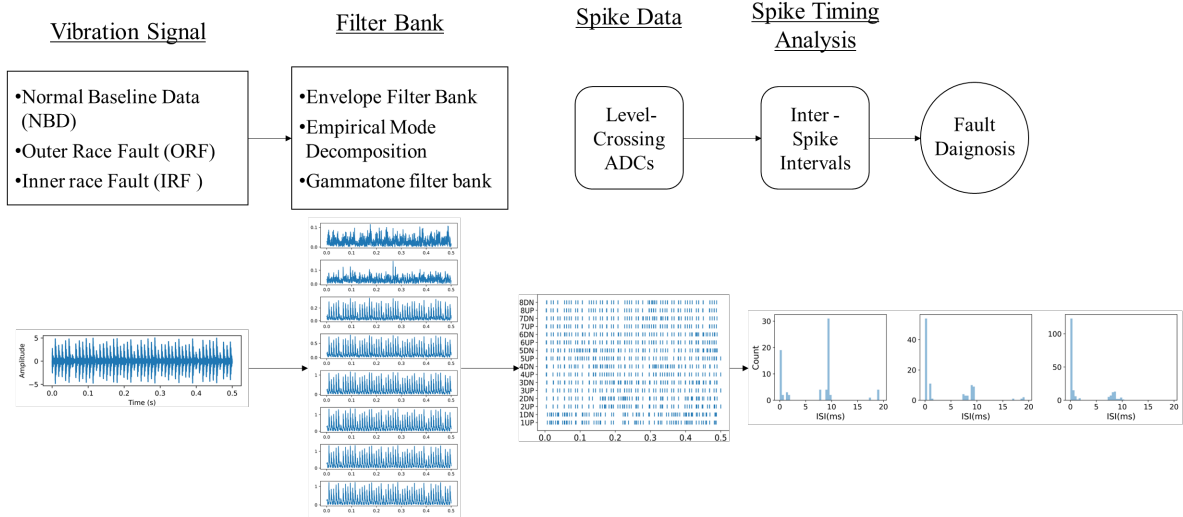


Figure 1. Schematic representation of the work.

The dataset consists of vibration signals categorized into four distinct classes of motor bearing faults: outer race fault (ORF), inner race fault (IRF), ball fault, and normal baseline data (NBD). These faults are introduced by electro-discharge machining to create fault diameters ranging from 0.1778 to 0.7112 mm on the rolling elements, inner and outer races. The braking torque by the dynamometer varies at four levels, leading to four different power levels of the motor, 0, 1, 2, and 3 horsepower while maintaining a constant motor speed, which are referred to as the four different load stages of the system. Specifically, the corresponding motor speeds for these torque levels are 1796, 1772, 1750, and 1730 revolutions per minute, respectively.

Table 1. Details of Data Used in the Analysis

Data Sets	Operating Details	
<ul style="list-style-type: none"> • Normal Baseline Data (NBD) • Outer Race Fault (ORF) • Inner Race Fault (IRF) 	Load-stage	2 Hp
	Motor speed	1750 RPM
	Sampling Frequency	48 kHz
	Sampling time	10 s
	Fault Diameter	0.1778 mm

The purpose of utilizing the CWRU dataset in this study is to establish a benchmark and facilitate standardized comparisons. The details of the selected datasets are outlined in Table 1. Among these datasets, there is one healthy dataset and two faulty datasets. This selection allows for a significant comparison between the faulty and normal datasets in terms of fault diagnosis. The dataset with a minimum fault diameter of 0.1778 mm is only selected here, as in Magar et al., 2021 to establish proof-of-concept of our proposed model. This way, the problems associated with other parts of the CWRU data set are avoided (Li et al., 2020; Smith & Randall, 2015; Yang et al., 2018).

2.2. Filters

Filter banks are utilized to decompose a signal, enabling the separation of its different frequency components. This allows for identifying and analyzing specific vibration patterns or anomalies with enhanced accuracy and clarity (Antoni, 2021b; Holguín-Londoño et al., 2016). This work decomposes the signals using an envelope, an empirical mode decomposition (EMD), and gammatone filter banks. These filters are analyzed to evaluate their compatibility and identify the most efficient filter for diagnosing faults in bearings based on vibration signals with the proposed approach. In this work, the analysis focuses on envelope and EMD filter banks due to their widespread usage in vibration signal decomposition. This approach allows for a standard comparison, enabling the comparison of both methods with the bio-inspired cochlea model, also known as the gamma tone filter bank.

2.2.1. Filter bank 1: Envelope.

An envelope filter bank is used in vibration signal processing of bearing to distinguish the impacts of faults from the noisy environment. It isolates the high-frequency component (related to bearing defects) from the low-frequency component (noise) (Randall & Antoni, 2011) (Wei et al., 2021). In the context of bearing analysis, the envelope signal reveals more defect information (periodic impacts of defects) than the raw signal (Chen et al., 2022; Tse et al., 2001). The envelope technique was used to decompose the 0-5kHz area into eight channels. Also, a cascade on the upper cut-off frequency of the band-pass filter was used before rectification and low-pass filtering.

2.2.2. Filter bank 2: Empirical Mode Decomposition (EMD).

The EMD filter banks are commonly used in bearings fault detection to decompose nonlinear and non-stationary signals into intrinsic mode functions (IMFs) (Huang et al., 1998). The input signal is decomposed into several IMF components through a sifting process, each representing an oscillatory signal component with a distinct time scale and band-limited nature (Dybała & Zimroz, 2014; Kumar et al., 2023). This process represents the original signal as a combination of IMFs and a low-order polynomial residue. Combining the IMF components with the residue can reconstruct the original signal using linear combination techniques (Van et al., 2014). Using the method proposed by Huang et al., 1998, the vibration measurements are decomposed into eight sets of intrinsic mode functions (IMFs).

2.2.3. Filter bank 3: Gammatone.

The gammatone filter bank, commonly utilized in audio signal processing and speech recognition, emulates the frequency analysis of the human auditory system (Slaney, 1993). Each filter within the bank captures energy within a specific frequency band, determined by its center frequency and bandwidth. These filters are essential for modeling the frequency filtering properties of the basilar membrane during cochleagram creation. Each overlapped filter corresponds to a specific position on the membrane. The cochleagram technique is known for its superior performance in robust feature extraction (Y. Zhang et al., 2022). By adjusting the central frequency, the filter bank captures information from various frequency bands, facilitating the extraction of harmonic features (Abdul et al., 2020). The purpose of including gammatone filters in this study is to evaluate the effectiveness of decomposing vibration signals for bearing fault diagnosis. A cascade of eight IIR (Infinite Impulse Response) filters with linearly spaced center frequencies is used to decompose the vibration measurements.

3. SPIKE ENCODING

In signal processing, the first step is the quantization of an analog signal in continuous time to obtain the digital representation. The conventional means to achieve the conversion is analog-to-digital converters (ADC). The recommended sampling rate in fault diagnosis of bearing is greater than $>40\text{kHz}$ for fault diagnosis of bearing (Smith & Randall, 2015b). Continuous or real-time monitoring of machines consumes energy in transmitting, processing, and storing large data. A bio-inspired, neuromorphic model based on event-driven (or level-crossing) principles is employed to address this issue and improve energy efficiency. This model effectively reduces the amount of data processed at the initial level, thereby minimizing power consumption. (Weltin-Wu & Tsvividis, 2013). The analog-to-spike conversion (delta encoding), based on the level-crossing analog-to-digital

converter (LC-ADCs), can efficiently convert continuous analog signals into digital representations. The LC-ADCs generate (up or down) events only when the change in signal is larger than the reference level (threshold), which gives remarkable compression properties (He et al., 2022; Safa et al., 2023). This adaptive sampling rate efficiently captures the signal's instantaneous spectral content. In sparse signals with an occasional high spectral range, fewer samples are needed compared to a Nyquist fixed-rate ADC, resulting in direct signal compression and reduced power consumption at the system level. The optimal sampling rate selection of LC-ADCs can affect data rate and power consumption (Saeed et al., 2021). The challenges in implementing LC-ADCs include generating false samples in the presence of noise and efficiently representing signals with high amplitude precision. The LC-ADCs can be optimized for efficient and accurate data conversion by applying noise rejection and adaptive precision techniques, see Ye et al., 2021 for an in-depth discussion. The average event rate is defined by the LC-ADCs threshold parameter so that it is above the maximum fault frequency of interest, this gives a maximum value on the threshold. Furthermore, we checked that the selected threshold is well above the noise floor, which gives a minimum possible value on the threshold. Thereby we aim to represent the relevant information in the signal using a minimum event rate. We investigated the effect of further increasing the event rate and found that this only contributes noise while the spectral peaks are still visible.

Understanding the encoded spike data information is crucial for investigating patterns in neuroscience (Karimov et al., 2022). A widely used tool for analyzing spike data is measuring the distance between spikes, known as the inter-spike interval (ISI). The ISI is calculated as the time difference between two consecutive spikes, representing the duration between successive spike occurrences, and stored as the ISI. This measure can be used to analyze burst activity in the spike train. The detection of bursts using spike intervals alone can be challenging at times. However, the ISI histogram method is found to be a quantitative, simpler, and more reliable approach for characterizing the differences between two types of activity patterns. (Cocatre-Zilgien & Delcomyn, 1992; Kaneoke & Vitek, 1996). The ISI histogram represents characteristics of firing activity, bursting behavior, and potential underlying mechanisms and is formed by the time binning of ISIs. In the representation of the ISI histogram, there are two regions for analyzing bursts: intra-burst (i.e., within burst) and inter-burst (i.e., between burst). It is important to note that there can be multiple bursts depending on the information conveyed by sensory input (Ishii & Hosoya, 2020).

4. RESULTS AND DISCUSSIONS

This section aims to verify the performance of the proposed approach for fault diagnosis using selected parts of the CWRU dataset. Specifically, the signals NBD (Normal

Baseline Data), ORF (Outer Race Fault), and IRF (Inner Race Fault), as discussed in Table 1, are sliced to obtain a sampling time of 0.5 seconds. This duration was selected based on the recommendation of a minimum of 20-25 repetitions of impulses in the selected signals (Strömbergsson, 2020). The slicing of these signals serves two purposes: reducing power consumption during subsequent processing and evaluating the effectiveness of the proposed method with minimal required data in machine condition monitoring. Figure 2 shows the sliced ORF data, and upon visual inspection, the minimum repetitive impulses required in the signal for vibration analysis can be verified. The same is done with NBD and IRF datasets, but only the ORF signals are presented here as one example of data to avoid redundant representations.

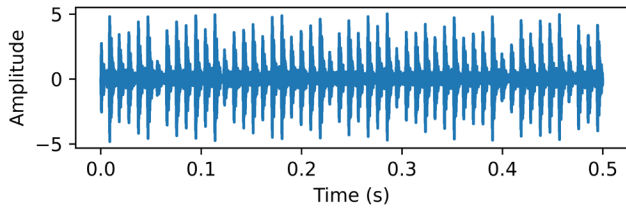


Figure 2. Vibration signal for ORF before filtering
All signals are processed to decompose in eight parts using an envelope, empirical mode decomposition (EMD), and gamma-tone filter bank. Each part represents each channel for further processing. So, there are eight channels for one type of Filter bank with one data set, meaning there are 8 X 3 channels for all three signals from each filter bank, and in all, there are 8 X 3 X 3 channels.

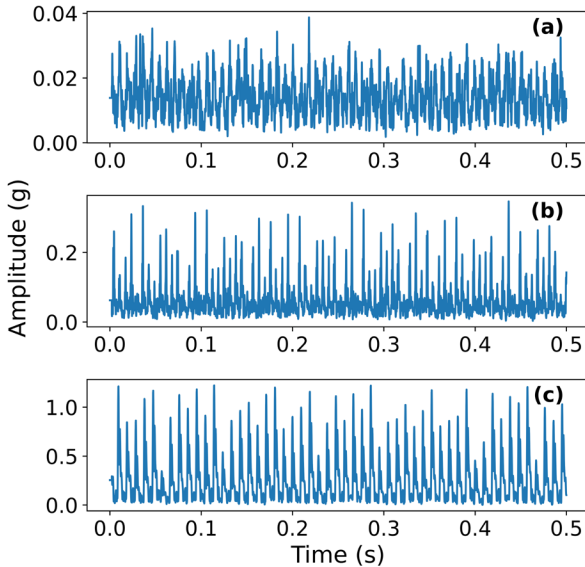


Figure 3. Decomposition result of 8th of envelope filter bank for (a) NBD, (b) ORF, and (c) IRF datasets.

It is not feasible to present all the output here, so only the signals obtained from the eighth channels of the envelope filter bank for all datasets are shown in Figure 3. This

selection of narrow-band components allows better visual comparisons across the datasets. The presence of repetitive impulses can be observed in all the datasets, and this verifies the impulses are caused by fault and noise from interference of the other components. The comparison of Figure 3(b) and Figure 2 shows that noise components are considerably reduced.

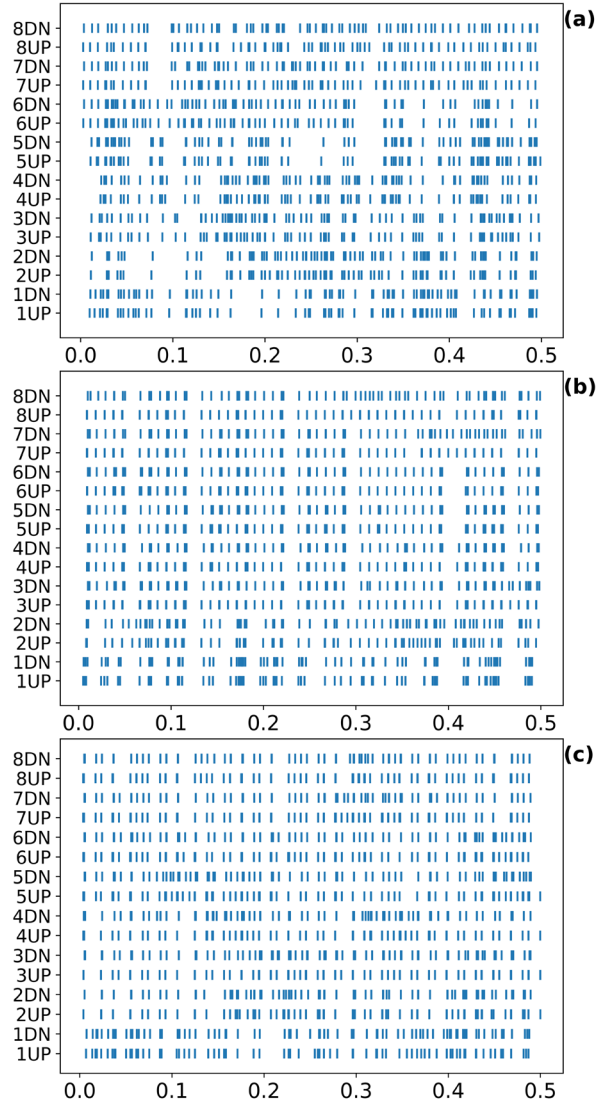


Figure 4. Spikes train using of (a) NBD, (b) ORF and (c) IRF datasets with envelope filter bank.

The spike train generated for each data set corresponding to different filters are obtained, but it is difficult to identify the fault by visual inspection of change in spike train. In this work, the inter-spike intervals (ISIs) of spike trains are investigated to understand better the filtering effects in bearing fault diagnosis. To further have a comparative analysis among all the signals, ISIs histograms are plotted. Figures 5, 6 and 7 represent the ISIs histogram for the NBD, ORF, and IRF datasets corresponding to the last channel of

all three filter banks. In Figures 5, 6, and 7, the count on the 'Y' axis represents the number of intervals.

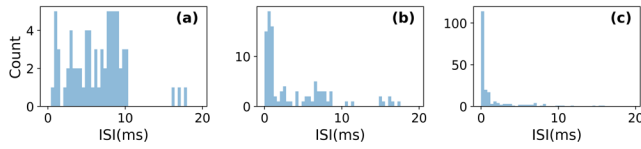


Figure 5. ISIs Histogram of NBD for (a) Envelope, (b) EMD, and (c) Gammatone filter banks

The high population of small-time intervals can be observed in a few numbers of bins, and large-time intervals are widespread over a large number of bins with low populations (Pasquale et al., 2010). For the NBD dataset, there is a number of peaks for the envelope filter bank in Figure 5(a), but there are a few peaks with EMD and gammatone filter banks shown in Figure 5(b) and Figure 5(c). This shows the distribution of spikes randomly over bins, which shows the presence of noise in signals.

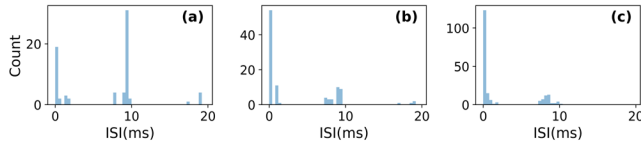


Figure 6. ISIs Histogram of ORF dataset for (a) Envelope, (b) EMD, and (c) Gammatone filter banks

Figure 6, represents the ISIs corresponding to the ORF dataset, t . The first peak is near 0 ms, which shows the intra-burst, while the second peak at 9 ms corresponds to the inter-burst (Cotterill & Eglén, 2018). The burst can be clearly observed and identified from the visual inspection of these figures. The second peak at 9 ms is present because of the outer race failure, which is related to the outer race fault frequency of 102 Hz. This shows that the developed method can diagnose the fault in the bearing using vibration signals.

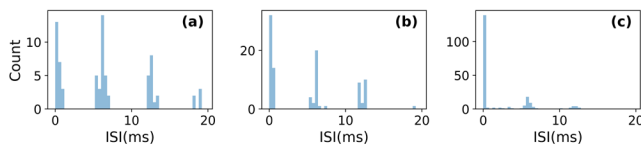


Figure 7. ISIs Histogram of IRF dataset for (a) Envelope, (b) EMD, and (c) Gammatone filter banks

The method can be further verified with another dataset, i.e., ORF. Figure 7 represents the ISIs corresponding to the ORF dataset, there are number of peaks in the with envelope filter bank, but few with the EMD and gammatone filter banks. But, the peaks show a repetition at an interval of 6 ms, which shows the presence of inner race fault and is equal to the fault frequency of 157.8 Hz. This shows the effectiveness of the proposed method in fault diagnosis of the bearing.

5. CONCLUSIONS

This work investigates alternative methods to generate event-based representations of condition monitoring vibration signals for bearing fault diagnosis. For the smallest (0.1778 mm) outer/inner race faults in the CWRU dataset, fault signatures are seen in spike interval statistics using all three investigated filter banks (EMD, Envelope, and Gammatone). However, only in the case of the envelope filter bank interspike intervals corresponding to bearing fault frequencies are dominant. Also, for the envelope filter bank this is the case for all channels, which is not the case for the other filter banks. These results demonstrate that the choice of filter bank is important in the design of LC-ADCs for event-based processing of condition monitoring vibration signals, as the number of events that need to be generated and processed to achieve the desired performance (signal-to-noise ratio, etc.) will influence the power consumption of the system. The LC-ADC with an average spike rate of 300 Hz is found to be sufficient to encode the fault information present in the signals considered here, provided that the filter transfer function is appropriately selected.

On the contrary, if an inappropriate filter is used, many of the generated events will encode information that is redundant or unrelated to the faults and render unnecessary energy costs for downstream processing. Thus, balancing between fault-specific solutions and generic systems that can generalize across machine and bearing types is a complex co-design problem that requires optimization of both the filter bank and the LC-ADCs with constraints from the applications.

ACKNOWLEDGMENT

This work is funded by the Jubilee Fund and Creaternity at the Luleå University of Technology, and the Kempe Foundation, contract numbers SMK21-0046 and JCSMK JF-2303.

REFERENCES

- Abdul, Z. K., Al-Talabani, A. K., & Ramadan, D. O. (2020). A Hybrid Temporal Feature for Gear Fault Diagnosis Using the Long Short Term Memory. *IEEE Sensors Journal*, 20(23), 14444–14452. <https://doi.org/10.1109/JSEN.2020.3007262>
- Ahmer, M., Sandin, F., Marklund, P., Gustafsson, M., & Berglund, K. (2022). Using Multivariate Quality Statistic for Maintenance Decision Support in a Bearing Ring Grinder. *Machines*, 10(9). <https://doi.org/10.3390/machines10090794>
- Antoni, J. (2021a). A Critical Overview of the “Filterbank-Feature-Decision” Methodology in Machine Condition Monitoring. *Acoustics Australia*, 49(2), 177–184. <https://doi.org/10.1007/s40857-021-00232-7>

- Antoni, J. (2021b). A Critical Overview of the “Filterbank-Feature-Decision” Methodology in Machine Condition Monitoring. *Acoustics Australia*, 49(2), 177–184. <https://doi.org/10.1007/s40857-021-00232-7>
- Attoui, I., Oudjani, B., Boutasseta, N., Fergani, N., Bouakkaz, M. S., & Bouraiou, A. (2020). Novel predictive features using a wrapper model for rolling bearing fault diagnosis based on vibration signal analysis. *International Journal of Advanced Manufacturing Technology*, 106(7–8), 3409–3435. <https://doi.org/10.1007/s00170-019-04729-4>
- Ault, T., & Bradley, T. (2022a). Risk-based approach for managing obsolescence for automation systems in heavy industries. *Systems Engineering*, 25(6), 551–560. <https://doi.org/10.1002/sys.21635>
- Ault, T., & Bradley, T. (2022b). Risk-based approach for managing obsolescence for automation systems in heavy industries. *Systems Engineering*, 25(6), 551–560. <https://doi.org/10.1002/sys.21635>
- Chen, B., Cheng, Y., Zhang, W., & Gu, F. (2022). Enhanced bearing fault diagnosis using integral envelope spectrum from spectral coherence normalized with feature energy. *Measurement: Journal of the International Measurement Confederation*, 189. <https://doi.org/10.1016/j.measurement.2021.110448>
- Cocatre-Zilgien, J. H., & Delcomyn, F. (1992). Identification of bursts in spike trains. In *Journal of Neuroscience Methods* (Vol. 41).
- Cotterill, E., & Eglén, S. J. (2018). *Burst detection methods*. <http://arxiv.org/abs/1802.01287>
- de Sá Só Martins, D. H. C., Viana, D. P., de Lima, A. A., Pinto, M. F., Tarrataca, L., Lopes e Silva, F., Gutiérrez, R. H. R., de Moura Prego, T., Monteiro, U. A. B. V., & Haddad, D. B. (2021). Diagnostic and severity analysis of combined failures composed by imbalance and misalignment in rotating machines. *International Journal of Advanced Manufacturing Technology*, 114(9–10), 3077–3092. <https://doi.org/10.1007/s00170-021-06873-2>
- Deepu, C. J., Xu, X. Y., Wong, D. L. T., Heng, C. H., & Lian, Y. (2018). A 2.3 μ W ECG-On-Chip for Wireless Wearable Sensors. *IEEE Transactions on Circuits and Systems II: Express Briefs*, 65(10), 1385–1389. <https://doi.org/10.1109/TCSII.2018.2861723>
- Dennler, N., Haessig, G., Cartiglia, M., & Indiveri, G. (2021). *Online Detection of Vibration Anomalies Using Balanced Spiking Neural Networks*. <http://arxiv.org/abs/2106.00687>
- Dybała, J., & Zimroz, R. (2014). Rolling bearing diagnosing method based on empirical mode decomposition of machine vibration signal. *Applied Acoustics*, 77, 195–203. <https://doi.org/10.1016/j.apacoust.2013.09.001>
- He, Y., Corradi, F., Shi, C., Ven, S. van der, Timmermans, M., Stuijt, J., Detterer, P., Harpe, P., Lindeboom, L., Hermeling, E., Langereis, G., Chicca, E., & Liu, Y. H. (2022). An Implantable Neuromorphic Sensing System Featuring Near-Sensor Computation and Send-on-Delta Transmission for Wireless Neural Sensing of Peripheral Nerves. *IEEE Journal of Solid-State Circuits*. <https://doi.org/10.1109/JSSC.2022.3193846>
- Hoang, D. T., & Kang, H. J. (2019). A survey on Deep Learning based bearing fault diagnosis. *Neurocomputing*, 335, 327–335. <https://doi.org/10.1016/j.neucom.2018.06.078>
- Holguín-Londoño, M., Cardona-Morales, O., Sierra-Alonso, E. F., Mejia-Henao, J. D., Orozco-Gutiérrez, Á., & Castellanos-Dominguez, G. (2016). Machine Fault Detection Based on Filter Bank Similarity Features Using Acoustic and Vibration Analysis. *Mathematical Problems in Engineering*, 2016. <https://doi.org/10.1155/2016/7906834>
- Huang, N. E., Shen, Z., Long, S. R., Wu, M. C., Shih, H. H., Zheng, Q., Yen, N.-C., Chao Tung, C., & Liu, H. H. (1998). The Empirical Mode Decomposition and the Hilbert Spectrum for Nonlinear and Non-Stationary Time Series Analysis. In *Source: Proceedings: Mathematical, Physical and Engineering Sciences* (Vol. 454). <https://www.jstor.org/stable/53161>
- Ingemarsdotter, E., Kambanou, M. L., Jamsin, E., Sakao, T., & Balkenende, R. (2021). Challenges and solutions in condition-based maintenance implementation - A multiple case study. *Journal of Cleaner Production*, 296. <https://doi.org/10.1016/j.jclepro.2021.126420>
- Ishii, T., & Hosoya, T. (2020). Interspike intervals within retinal spike bursts combinatorially encode multiple stimulus features. *PLoS Computational Biology*, 16(11). <https://doi.org/10.1371/journal.pcbi.1007726>
- Kaneoke, Y., & Vitek, J. L. (1996). Burst and oscillation as disparate neuronal properties. In *Journal of Neuroscience Methods* (Vol. 68).
- Karimov, T., Druzhina, O., Karimov, A., Tutueva, A., Ostrovskii, V., Rybin, V., & Butusov, D. (2022). Single-coil metal detector based on spiking chaotic oscillator. *Nonlinear Dynamics*, 107(1), 1295–1312. <https://doi.org/10.1007/s11071-021-07062-2>

- Kumar, A., Berrouche, Y., Zimroz, R., Vashishtha, G., Chauhan, S., Gandhi, C. P., Tang, H., & Xiang, J. (2023). Non-parametric Ensemble Empirical Mode Decomposition for extracting weak features to identify bearing defects. *Measurement: Journal of the International Measurement Confederation*, 211. <https://doi.org/10.1016/j.measurement.2023.112615>
- Kumar, A., Parkash, C., Vashishtha, G., Tang, H., Kundu, P., & Xiang, J. (2022). State-space modeling and novel entropy-based health indicator for dynamic degradation monitoring of rolling element bearing. *Reliability Engineering and System Safety*, 221. <https://doi.org/10.1016/j.ress.2022.108356>
- Kuncan, M., Kaplan, K., Minaz, M. R., Kaya, Y., & Ertunç, H. M. (2020). A novel feature extraction method for bearing fault classification with one dimensional ternary patterns. *ISA Transactions*, 100, 346–357. <https://doi.org/10.1016/j.isatra.2019.11.006>
- Li, J., Ashraf, A., Cardiff, B., Panicker, R. C., Lian, Y., & John, D. (2020). Low Power Optimisations for IoT Wearable Sensors Based on Evaluation of Nine QRS Detection Algorithms. *IEEE Open Journal of Circuits and Systems*, 1, 115–123. <https://doi.org/10.1109/ojcas.2020.3009822>
- Loparo, K. A. . (2012). *Case western reserve university bearing data center*. Case Western Reserve University. <https://engineering.case.edu/bearingdatacenter>
- MarketsandMarkets. (2023). *Oil Condition Monitoring Market*. <https://www.marketsandmarkets.com/Market-Reports/machine-health-monitoring-market-29627363.html>
- Miao, Y., Zhang, B., Lin, J., Zhao, M., Liu, H., Liu, Z., & Li, H. (2022). A review on the application of blind deconvolution in machinery fault diagnosis. *Mechanical Systems and Signal Processing*, 163. <https://doi.org/10.1016/j.ymsp.2021.108202>
- Mohammed, O. D., & Rantatalo, M. (2020). Gear fault models and dynamics-based modelling for gear fault detection – A review. In *Engineering Failure Analysis* (Vol. 117). Elsevier Ltd. <https://doi.org/10.1016/j.engfailanal.2020.104798>
- Nguyen, K. T. P., Medjaher, K., & Tran, D. T. (2022). A review of artificial intelligence methods for engineering prognostics and health management with implementation guidelines. *Artificial Intelligence Review*. <https://doi.org/10.1007/s10462-022-10260-y>
- Pasquale, V., Martinoia, S., & Chiappalone, M. (2010). A self-adapting approach for the detection of bursts and network bursts in neuronal cultures. *Journal of Computational Neuroscience*, 29(1–2), 213–229. <https://doi.org/10.1007/s10827-009-0175-1>
- Peeters, C., Antoni, J., & Helsen, J. (2020). Blind filters based on envelope spectrum sparsity indicators for bearing and gear vibration-based condition monitoring. *Mechanical Systems and Signal Processing*, 138. <https://doi.org/10.1016/j.ymsp.2019.106556>
- Quiñones-Grueiro, M., Prieto-Moreno, A., Verde, C., & Llanes-Santiago, O. (2019). Data-driven monitoring of multimode continuous processes: A review. In *Chemometrics and Intelligent Laboratory Systems* (Vol. 189, pp. 56–71). Elsevier. <https://doi.org/10.1016/j.chemolab.2019.03.012>
- Randall, R. B., & Antoni, J. (2011). Rolling element bearing diagnostics-A tutorial. In *Mechanical Systems and Signal Processing* (Vol. 25, Issue 2, pp. 485–520). Academic Press. <https://doi.org/10.1016/j.ymsp.2010.07.017>
- Saeed, M., Wang, Q., Martens, O., Larras, B., Frappe, A., Cardiff, B., & John, D. (2021). Evaluation of Level-Crossing ADCs for Event-Driven ECG Classification. *IEEE Transactions on Biomedical Circuits and Systems*, 15(6), 1129–1139. <https://doi.org/10.1109/TBCAS.2021.3136206>
- Safa, A., Van Assche, J., Frenkel, C., Bourdoux, A., Catthoor, F., & Gielen, G. (2023). Exploring Information-Theoretic Criteria to Accelerate the Tuning of Neuromorphic Level-Crossing ADCs. *ACM International Conference Proceeding Series*, 63–70. <https://doi.org/10.1145/3584954.3584994>
- Sahu, P. K., & Rai, R. N. (2022). Fault Diagnosis of Rolling Bearing Based on an Improved Denoising Technique Using Complete Ensemble Empirical Mode Decomposition and Adaptive Thresholding Method. *Journal of Vibration Engineering and Technologies*. <https://doi.org/10.1007/s42417-022-00591-z>
- Slaney, M. (1993). *An Efficient Implementation of the Patterson-Holdsworth Auditory Filter Bank*.
- Smith, W. A., & Randall, R. B. (2015a). Rolling element bearing diagnostics using the Case Western Reserve University data: A benchmark study. In *Mechanical Systems and Signal Processing* (Vols. 64–65, pp. 100–131). Academic Press. <https://doi.org/10.1016/j.ymsp.2015.04.021>
- Smith, W. A., & Randall, R. B. (2015b). Rolling element bearing diagnostics using the Case Western Reserve University data: A benchmark

- study. In *Mechanical Systems and Signal Processing* (Vols. 64–65, pp. 100–131). Academic Press. <https://doi.org/10.1016/j.ymssp.2015.04.021>
- Strömbergsson, D., Marklund, P., & Berglund, K. (2021). Multi-body simulation and validation of fault vibrations from rolling-element bearings. *Proceedings of the Institution of Mechanical Engineers, Part J: Journal of Engineering Tribology*, 235(9), 1834–1841. <https://doi.org/10.1177/1350650120977974>
- Strömbergsson, D., Marklund, P., Berglund, K., & Larsson, P. E. (2020). Bearing monitoring in the wind turbine drivetrain: A comparative study of the FFT and wavelet transforms. *Wind Energy*, 23(6), 1381–1393. <https://doi.org/10.1002/we.2491>
- Tse, P. W., Peng, Y. H., & Yam, R. (2001). Wavelet analysis and envelope detection for rolling element bearing fault diagnosis—their effectiveness and flexibilities. *Journal of Vibration and Acoustics, Transactions of the ASME*, 123(3), 303–310. <https://doi.org/10.1115/1.1379745>
- uit het Broek, M. A. J., Teunter, R. H., de Jonge, B., & Veldman, J. (2021). Joint condition-based maintenance and condition-based production optimization. *Reliability Engineering and System Safety*, 214. <https://doi.org/10.1016/j.res.2021.107743>
- Van Assche, J., & Gielen, G. (2020). Power Efficiency Comparison of Event-Driven and Fixed-Rate Signal Conversion and Compression for Biomedical Applications. *IEEE Transactions on Biomedical Circuits and Systems*, 14(4), 746–756. <https://doi.org/10.1109/TBCAS.2020.3009027>
- Van, M., Kang, H. J., & hin, K. S. (2014). Rolling element bearing fault diagnosis based on non-local means de-noising and empirical mode decomposition. *IET Science, Measurement and Technology*, 8(6), 571–578. <https://doi.org/10.1049/iet-smt.2014.0023>
- Wang, T., Liu, H., Guo, D., & Sun, X. M. (2023). Continual deep residual reservoir computing for remaining useful life prediction. *IEEE Transactions on Industrial Informatics*. <https://doi.org/10.1109/TII.2023.3271661>
- Wei, S., Wang, D., Wang, H., & Peng, Z. (2021). Time-Varying Envelope Filtering for Exhibiting Space Bearing Cage Fault Features. *IEEE Transactions on Instrumentation and Measurement*, 70. <https://doi.org/10.1109/TIM.2020.3033061>
- Weltin-Wu, C., & Tsividis, Y. (2013). An event-driven clockless level-crossing ADC with signal-dependent adaptive resolution. *IEEE Journal of Solid-State Circuits*, 48(9), 2180–2190. <https://doi.org/10.1109/JSSC.2013.2262738>
- Yeardley, A. S., Ejeh, J. O., Allen, L., Brown, S. F., & Cordiner, J. (2022). Integrating machine learning techniques into optimal maintenance scheduling. *Computers and Chemical Engineering*, 166. <https://doi.org/10.1016/j.compchemeng.2022.107958>
- Yu, J., Huang, J., Liu, C., & Xia, B. (2022). Fault Feature of Gearbox Vibration Signals Based on Morphological Filter Dynamic Convolution Autoencoder. *IEEE Sensors Journal*, 22(23), 22931–22942. <https://doi.org/10.1109/JSEN.2022.3213783>
- Zabin, M., Choi, H. J., & Uddin, J. (2023). Hybrid deep transfer learning architecture for industrial fault diagnosis using Hilbert transform and DCNN–LSTM. *Journal of Supercomputing*, 79(5), 5181–5200. <https://doi.org/10.1007/s11227-022-04830-8>
- Zhang, D., Chen, Y., Guo, F., Karimi, H. R., Dong, H., & Xuan, Q. (2021). A New Interpretable Learning Method for Fault Diagnosis of Rolling Bearings. *IEEE Transactions on Instrumentation and Measurement*, 70. <https://doi.org/10.1109/TIM.2020.3043873>
- Zhang, K., Xu, Y., Liao, Z., Song, L., & Chen, P. (2021). A novel Fast Entrogram and its applications in rolling bearing fault diagnosis. *Mechanical Systems and Signal Processing*, 154. <https://doi.org/10.1016/j.ymssp.2020.107582>
- Zhang, X., Zhao, B., & Lin, Y. (2021). Machine Learning Based Bearing Fault Diagnosis Using the Case Western Reserve University Data: A Review. In *IEEE Access* (Vol. 9, pp. 155598–155608). Institute of Electrical and Electronics Engineers Inc. <https://doi.org/10.1109/ACCESS.2021.3128669>
- Zhang, Y., Dora, S., Martinez-Garcia, M., & Bhattacharyaand, S. (2022). Machine Hearing for Industrial Acoustic Monitoring using Cochleagram and Spiking Neural Network. *IEEE/ASME International Conference on Advanced Intelligent Mechatronics, AIM, 2022-July*, 1047–1051. <https://doi.org/10.1109/AIM52237.2022.9863412>
- Zuo, L., Xu, F., Zhang, C., Xiahou, T., & Liu, Y. (2022). A multi-layer spiking neural network-based approach to bearing fault diagnosis. *Reliability Engineering and System Safety*, 225. <https://doi.org/10.1016/j.res.2022.108561>